ISSN 1028-334X, Doklady Earth Sciences, 2006, Vol. 409, No. 5, pp. 824–830. © Pleiades Publishing, Inc., 2006.
Original Russian Text © V.F. Polin, A.I. Khanchuk, S.I. Dril, G.P. Sandimirova, L.S. Tsurikova, 2006, published in Doklady Akademii Nauk, 2006, Vol. 409, No. 2, pp. 241–247.

GEOPHYSICS

Petrogenesis of Gold-Bearing Dioritoids of the Ketkap–Yuna Magmatic Province, Aldan Shield

V. F. Polin[a], Corresponding Member of the RAS A. I. Khanchuk[a], S. I. Dril[b], G. P. Sandimirova[b], and L. S. Tsurikova[a]

Received October 28, 2005

DOI: 10.1134/S1028334X06050333

Significant volumes of subalkaline magmatic rocks in the continental crust of the Aldan Shield raises problems concerning their sources in the context of geodynamics, continental growth, and crustal recycling [1, 3, and others]. Our research was aimed at petrogeochemical and geodynamic typification of the Jurassic–Early Cretaceous Uchur (Oblachnyi) Complex of subalkaline trachyandesite–diorite–granodiorites in order to decipher its tectonic setting and petrogenesis. The Uchur Complex is developed in the Ketkap–Yuna magmatic province, which represents a zone of Late Mesozoic tectonomagmatic activation of the shield. This issue is also of practical interest, because subalkaline quartz diorites of the third phase of this complex host economic gold mineralization.

The diversity of Mesozoic igneous rocks in the Aldan Shield is related to two large tectonomagmatic cycles, which are subdivided by different authors into three to five stages. We hold a two-cycle and five-stage scheme for the Ketkap–Yuna province [5]. The first cycle was responsible for the formation of the low-volume trachydacite–trachyandesite association and emplacement of sill-shaped bodies of the first and second phases of comagmatic subalkaline diorite–granodiorite association (first and second stages of magmatism) (Table 1). These associations are combined [5] into the Uchur Complex.

The emplacement of the subalkaline diorite–granodiorite association (third and fourth stages of the Uchur Complex) was completed during the second cycle (third and fourth stages) of Mesozoic magmatism. Simultaneously, the Bokur volcanoplutonic alkaline complex [6] and Dar'ya plutonic alkaline complex [7] were formed. Termination of alkaline magmatic activity was followed by the emplacement of the trachydacite–monzonite–syenite association (Ketkap Complex) at the western flank of the Ketkap magmatic uplift. Small volumes of the Ketkap monzonitoids are encountered among other massifs of the Ketkap–Yuna province in close association with alkaline potassic rocks of the Dar'ya Complex. The fifth stage of Mesozoic magmatism was marked by the emplacement of a dike series of alkaline and subalkaline potassic rocks of the Dar'ya and Ketkap complexes, respectively.

Geological and petrographic characteristics of the Uchur Complex are reported in [5] and other publications. In this paper, we report representative petrochemical, trace element, and isotopic compositions of rocks and results of their petrogeochemical and geodynamic interpretation (Table 2).

Dioritoids of the Uchur Complex are arbitrarily classified as subalkaline diorites, quartz diorites, and granodiorites, as well as moderately silicic granites (Tables 1, 2). Volcanic facies are represented by trachyandesites and trachydacites. Dikes and veins consist of trachyandesites, diorites, odinites, spessartites, and occasional vogesites, leucogranites, and gabbroids [5 and others].

Basic, intermediate, and moderately silicic rocks of the complex are ascribed to sodic, high-Ca, high-Fe, and Mg–Fe metaluminous series, while silicic rocks are ascribed to peraluminous series. The total alkalinity and calc-alkaline balance (Peacock index 56) indicate that the Uchur rocks are intermediate between calc-alkaline and subalkaline series. As compared to the first stage, the magmatic rocks of the second stage exhibit higher K content (consequently, higher alkalinity), with the most silicic rocks grading into subalkaline series (Table 2).

The rocks of the Uchur Complex typically have high Ba and Sr contents (Table 2). Therefore, they can be ascribed to the latite geochemical type, which is often interpreted by some modern researchers as products of alkaline basaltic magmas generated in a superplume or riftogenic setting. At the same time, this complex shows suprasubduction signatures: moderate to significant

[a] Far East Geological Institute, Far East Division, Russian Academy of Sciences, pr. Stoletiya Vladivostoka 159, Vladivostok, 690022 Russia; e-mail: vfpolin@mail.ru

[b] Vinogradov Institute of Geochemistry, Siberian Division, Russian Academy of Sciences, ul. Favorskogo 1a, Irkutsk, 664033 Russia; e-mail: sdril@igc.irk.ru

Table 1. Evolution of Mesozoic magmatism of the Uchur Complex in the Ketkap–Yuna province

Cycle	Association	
	trachyandesite–trachydacite	subalkaline diorite–granodiorite
	magmatic phases, absolute age of the rocks	
Second	Absent	**Fourth (K_1)** (138; 120 ± 3 Ma) Small stocks and laccoliths, occasionally dikes and thin sills of subalkaline granites and subalkaline granodiorite–quartz syenites
	Absent	**Third** (J_3–K_1) (137, 138, 138, 130 ± 20 Ma) Large laccoliths, thick sills, more rarely, small stocks of subalkaline quartz diorites and diorite porphyrites; thin sills and rare dikes of pyroxene tarchyandesites, Fe-rich gabbros, sill-shaped bodies and lenses of gabbrodiorites and gabbro pegmatites
First	**Second** Short lava flows and thin horizons of trachydacite tuffs; sills and extrusive domes, more rarely, dikes of trachydacites and trachyrhyodacites (along the subsidence caldera periphery)	**Second** (J_2–J_3) (155, 151 ± 5 Ma) Thin to moderately thick sills of syenite porphyries and subalkaline granodiorite porphyries
	First Thin horizons of tuffs, tuffolavas, and lavas of andesites and tarchyandesites (in subsidence calderas); small sills and rare dikes of the same rocks	**First** (J_1–J_2) (167, 172, 183, 188 Ma) Thin sills of subalkaline quartz-bearing and quartz-free diorite porphyrites, rare dikes and thin sill spessartites, vogesites

Note: Absolute age data are adopted from materials of geological survey.

enrichment in some LILE and LREE relative to HREE; negative Nb–Ta anomalies; moderate to low contents of K_2O, Rb, U, Th, and HFSE; and high Ba/Nb, Th/Ta, Zr/Nb, Ba/La, and La/Ta ratios. In addition, they are characterized by the absence of an Eu minimum and significant LREE fractionation at weak HREE fractionation, which is typical of tonalite–trondhjemite and some alkaline potassic associations developed at the old shields [1, 6, 7, and others]. Most rocks of the Uchur Complex bear signatures of tonalite–trondhjemite and monzonite–syenite series. The shape of spidergrams is similar for most rocks of the complex (Fig. 1), indicating their genetic affinity.

Petrogeochemical typification with the application of various diagrams and calculation methods [1–13 and others] showed that the Uchur magmatic rocks are similar to the postcollisional, late orogenic, and postorogenic granitoids of continental volcanic arcs. In particular, data points in the Pearce diagrams are plotted in the field of volcanic-arc granitoids near the average composition of *I*-type granites. The studied granitoids reveal petrogeochemical features of *M*- and *I*-type granites, while the most silicic rocks approximate *S*-granites. In the discriminant diagram of Velikoslavinsky, the Uchur subalkaline granites, leucogranodiorites, and granodiorites are plotted in the field of island-arc (suprasubduction) granites near the boundary with collisional granitoids. The position of data points in the diagrams of Fershtater and Nedashkovsky indicates their affiliation to "monzonite-latites," "mantle magma differentiates," and "continental andesite derivatives" types. In the diagram of Rub and Datsenko, most rocks of the complex occupy the field of mantle-derived magmas, which is typical of the trachyandesite–monzonite (latite) associations. The Uchur granitoid field is located between the curves for calc-alkaline series of active continental margins and rocks of continental rift zones. Data points of subalkaline diorites are confined to the curve of rift zones. When compared with schemes of petrochemical typification of granitoid associations [4, 10–13, and others], the Uchur rocks demonstrate combination of features of palingenic granitoids and granitoids derived from basaltic and alkaline basaltic magmas (Fig. 2).

All aforementioned data indicate that the studied complex possesses hybrid geochemical characteristics, which are transitional between suprasubduction and within-plate types. This complex bears specific features of latite-series rocks, on the one hand, and approximates continental volcanic arcs, on the other hand. Such a composition requires explanation.

Existing models of Mesozoic magmatism in the Aldan Shield are based on its relation either with collision between the East Siberian and Chinese plates [3 and others] or with the Californian-type (continental transform margin) setting [6, 7, 9]. Indications of its superplume nature are also available [1, 2, 6, 7, and others].

Based on geological and petrogeochemical data, the parental melts of the Uchur Complex of the Ketkap–Yuna province were presumably generated by partial

Table 2. Chemical and trace element composition of representative samples of the typical rocks of the Uchur Complex of the Ketkap–Yuna province

Component	PN-250-2501A Odinite	PN-9266-1 Malkhite	PN-238-8642 Subalkaline quartz diorite	PN-139-1612 Subalkaline quartz diorite	PN-138-1595 Trachyandesite	PN-137-1567 Subalkaline leucogranodiorite	PN-9260-6 Subalkaline granodiorite	PN-174-8199 Melanocratic amphibole gabbro	PN-M62-0214 Subalkaline gabbro
	(1)*	(1)	(1)	(1)	(1)	(2)	(2)	(3)	(3)
	1**	2	3	4	5	6	7	8	9
SiO_2	50.57	55.30	59.64	61.42	61.46	65.03	65.74	43.64	47.13
TiO_2	1.45	0.80	0.56	0.55	0.63	0.20	0.27	1.14	1.13
Al_2O_3	15.12	16.804	18.59	16.78	17.94	17.48	17.72	18.26	18.08
Fe_2O_3	3.21	4.00	3.31	3.60	2.07	0.96	1.56	8.46	6.93
FeO	6.09	4.70	3.01	1.86	3.14	0.48	1.14	6.09	4.97
MnO	0.09	0.14	0.10	0.11	0.11	0.06	0.07	0.16	0.22
MgO	6.74	4.40	1.57	1.82	1.57	0.40	1.04	5.02	3.43
CaO	9.86	6.60	6.01	5.21	3.99	3.08	4.05	11.56	12.02
Na_2O	2.80	3.90	4.35	4.53	4.25	5.47	5.13	2.76	3.70
K_2O	1.05	2.30	2.50	2.13	3.88	2.89	2.37	0.92	0.71
P_2O_5	0.64	0.30	0.25	0.21	0.23	0.05	0.23	0.73	0.86
H_2O	0.07	0.10	0.01	0.08	0.08	0.03	0.02	0.08	0.12
LOI	1.89	0.70	0.19	1.35	0.25	3.67	0.28	0.68	0.48
Series***	CA(M)	CA(M)	CA(M)	CA(M)	CA(M)	CA(L)	CA(L)	CA(M)	CA(M)
Cr	138	150	20	36	79	11	15	18	28
Ni	60	25	18	20	6	6	6	32	13
Co	36	28	10	11	7	2	5	33	21
V	307	160	130	121	210	40	48	250	283
Rb	60	33	46	50	91	58	42	15	11
Cs	0.96	0.64	0.72	0.83	7.84	0.96	0.49	0.62	0.66
Ba	247	378	463	816	787	1104	750	113	303
Sr	699	736	754	1334	855	352	1318	1916	1745
Ta	0.7	0.20	0.15	0.56	0.47	0.08	0.07	0.31	0.24
Nb	5.1	4.80	8.3	9.1	9.7	6.40	4.70	5.3	3.31
Hf	1.6	2.15	3.09	2.05	3.07	1.40	0.75	2.13	1.70
Zr	34	82	123	139	123	143	122	146	44.26
Y	25	21	24	20	16	8	7	27	20.84
Th	1.57	1.61	2.38	3.28	4.74	0.74	1.27	0.86	0.60
U	0.65	0.57	1.11	1.27	1.51	0.56	0.58	0.36	0.22
La	19.42	15.24	18.36	33.60	19.86	7.51	7.42	21.74	22.62
Ce	37.08	37.37	45.78	60.73	52.41	15.35	18.27	50.01	59.58
Pr	6.03	4.76	5.19	8.03	4.91	1.83	2.06	9.22	8.16
Nd	25.63	23.52	23.18	36.06	20.64	8.02	9.39	39.76	38.07
Sm	5.72	4.94	4.81	6.51	3.92	1.54	1.83	8.19	7.94
Eu	1.81	1.46	1.43	1.80	1.12	0.58	0.64	2.42	2.78
Gd	5.34	4.13	4.10	4.87	3.29	1.41	1.47	6.87	7.00
Tb	0.80	0.66	0.67	0.76	0.48	0.19	0.22	0.97	0.92
Dy	4.27	3.51	3.82	3.70	2.71	1.16	1.13	4.88	4.98
Ho	0.84	0.67	0.78	0.67	0.50	0.22	0.20	0.92	0.83
Er	2.22	1.96	2.32	1.87	1.52	0.71	0.59	4.91	2.29
Tm	0.37	0.28	0.36	0.27	0.23	0.12	0.09	0.39	0.30
Yb	1.91	1.72	2.19	1.87	1.50	0.70	0.54	2.08	1.74
Lu	0.28	0.28	0.33	0.24	0.23	0.10	0.07	0.32	0.22
B	11.08	8.00	6.00	14.00	6.00	23.00	5.00	9.00	–
Eu/Eu*	1.00	0.99	0.98	0.98	0.95	1.20	1.19	0.99	1.14
Rb/Sr	0.09	0.05	0.06	0.04	0.11	0.16	0.03	0.01	0.01
La/Ta	27.74	76.20	122.40	60.00	42.25	93.88	63.14	70.13	94.25
Th/Ta	2.24	8.05	15.87	5.86	10.08	9.25	18.14	2.77	2.50
Ba/Nb	49.40	78.75	55.78	89.67	81.13	172.50	159.57	21.32	91.54
Zr/Nb	6.8	17.08	14.82	15.27	12.68	22.34	25.96	27.55	13.29
$^{87}Sr/^{86}Sr$	–	–	0.704350	–	–	–	0.704420	–	–
ΣTR + Y	353.19	121.5	137.32	180.98	129.32	47.41	50.92	179.68	178.43

Table 2. (Contd.)

Component	PN-045-6184 Subalkaline gabbrodiorite	PN-137-1577 Subalkaline diorite	PN-165-1776 Subalkaline quartz diorite	PN-142-8126 Subalkaline quartz diorite	PN-174-8122 Subalkaline quartz diorite	PN-157-1711 Subalkaline quartz diorite	PN-244-8584 Subalkaline quartz diorite	PN-68,2-8154A Subalkaline granodiorite	PN-238-8618 Subalkaline leucogranodiorite	PN-142-8112 Subalkaline leucogranodiorite
	(3)	(3)	(3)	(3)	(3)	(3)	(3)	(4)	(4)	(4)
	10	11	12	13	14	15	16	17	18	19
SiO_2	52.13	57.26	59.92	59.20	59.78	56.23	59.90	64.25	67.63	67.50
TiO_2	1.07	0.67	0.55	0.66	0.62	0.82	0.57	0.62	0.30	0.25
Al_2O_3	15.90	17.77	17.31	18.35	17.94	18.15	18.41	15.90	17.02	16.64
Fe_2O_3	6.55	3.25	3.74	3.60	4.06	4.23	3.67	2.76	1.38	1.36
FeO	4.56	3.00	2.26	2.49	2.00	3.23	2.69	2.49	1.03	0.88
MnO	0.15	0.01	0.18	0.13	0.12	0.16	0.12	0.07	0.06	0.05
MgO	4.42	2.20	1.46	1.70	1.68	2.21	1.72	1.04	0.71	0.40
CaO	7.46	7.44	6.16	5.86	5.60	7.04	5.51	3.97	3.49	3.12
Na_2O	3.79	4.20	4.27	4.43	5.01	4.18	4.25	3.96	4.93	4.03
K_2O	2.41	3.32	2.87	2.72	2.72	2.51	2.16	3.74	2.72	4.97
P_2O_5	0.50	0.31	0.32	0.28	0.26	0.45	0.24	0.32	0.12	0.06
H_2O	0.08	0.10	0.10	0.10	0.05	0.16	0.08	0.15	0.07	0.8
LOI	0.50	0.56	0.40	0.25	0.08	0.30	0.18	0.54	0.20	0.0
Series***	CA(M)	CA(M)	CA(M)	CA(M)	CA(M)	CA(M)	CA(M)	SA(M)	CA(M)	SA(M)
Cr	37	17	13	10	16	14	10	15	15	39
Ni	17	6	11	8	11	11	8	13	12	19
Co	23	5	14	16	13	11	12	6	9	2.4
V	320	113	83	150	140	119	120	62	85	26
Rb	52	114	65	80	67	55	61	88	55	129
Cs	0.87	–	1.11	1.51	1.19	0.81	0.68	0.93	0.55	2.36
Ba	585	1191	776	449	487	754	427	636	866	1035
Sr	998	1540	1173	1072	1212	1203	857	552	1101	766
Ta	0.41	–	0.46	0.36	0.38	0.61	0.60	0.60	0.40	0.86
Nb	6.20	10.00	7.5	7.3	7.8	8.1	6.5	9.07	5.7	8.53
Hf	1.22	–	1.05	1.13	1.19	1.69	1.73	2.22	0.91	1.65
Zr	29	168	190	160	124	29	131	63	150	42
Y	16	27	25	20	22	24	24	15	11	11
Th	2.29	–	4.00	3.59	4.81	4.27	3.48	5.39	2.54	7.03
U	0.85	–	0.85	1.46	1.64	1.55	1.74	1.66	1.10	1.36
La	23.58	32.00	37.05	20.28	32.87	41.04	23.98	27.95	13.58	35.81
Ce	52.56	68.00	68.28	52.24	59.99	91.92	43.66	59.50	25.16	67.69
Pr	6.52	–	8.93	6.91	8.05	10.64	6.89	6.64	3.72	6.52
Nd	27.47	36.00	39.32	32.00	36.60	43.59	25.57	25.54	13.92	24.75
Sm	5.30	–	7.2	6.2	6.81	8.14	5.13	4.47	2.66	3.74
Eu	1.75	–	2.03	1.84	1.91	2.34	1.59	1.29	0.90	0.96
Gd	5.21	–	5.45	4.67	5.25	6.81	4.57	4.17	2.18	3.02
Tb	0.62	–	0.86	0.75	0.79	0.93	0.71	0.56	0.30	0.36
Dy	3.71	–	4.43	3.61	4.04	5.64	3.81	3.59	1.71	2.48
Ho	0.66	–	0.85	0.67	0.75	1.04	0.77	0.69	0.33	0.47
Er	1.87	–	2.48	1.91	2.15	2.91	2.27	1.84	0.95	1.27
Tm	0.23	–	0.40	0.29	0.34	0.45	0.39	0.29	0.18	0.21
Yb	1.49	–	2.49	1.93	2.12	2.80	2.19	1.76	0.96	1.37
Lu	0.20	–	0.39	0.28	0.29	0.35	0.34	0.23	0.15	0.20
B	–	10.00	11.00	11.00	22.00	–	5.00	10.00	5.00	–
Eu/Eu*	1.02	–	0.99	1.04	0.98	0.96	1.00	0.91	1.14	0.87
Rb/Sr	0.05	0.07	0.06	0.07	0.06	0.05	0.07	0.16	0.05	0.17
La/Ta	57.51	–	80.54	56.33	86.50	67.28	39.97	46.58	33.95	41.64
Th/Ta	5.59	–	8.69	9*.97	12.66	7.00	5.80	8.98	6.35	8.17
Ba/Nb	94.35	119.1	103.48	61.50	62.44	93.09	65.69	70.12	151.93	121.34
Zr/Nb	4.68	16.80	4.08	21.92	15.90	3.58	20.15	6.95	26.32	4.92
$^{87}Sr/^{86}Sr$	–	–	–	0.704420	–	–	–	–	0.704410	–
ΣTR + Y	147.17	>163.0	205.16	162.58	262.17	242.6	145.87	153.52	77.7	159.85

Note: Oxides are given in wt %; others, in ppm. Legend: (*) Magmatic phase; (**) ordinal number of sample; (***) petrochemical series (after [4]): (CA) calc-alkaline, (SA) subalkaline; subtypes (in parentheses): (M) moderately alkaline, (L) low-alkaline. Chemical analyses were performed at the Far East Geological Institute, Vladivostok (L. I. Alekseeva, analyst). REE and trace elements were analyzed by the ICP-MS method at the Vinogradov Institute of Geochemistry and Analytical Chemistry, Irkutsk (E. B. Smirnova, G. P. Sandimirova, and V. I. Lozhkin, analysts). (–) Not determined.

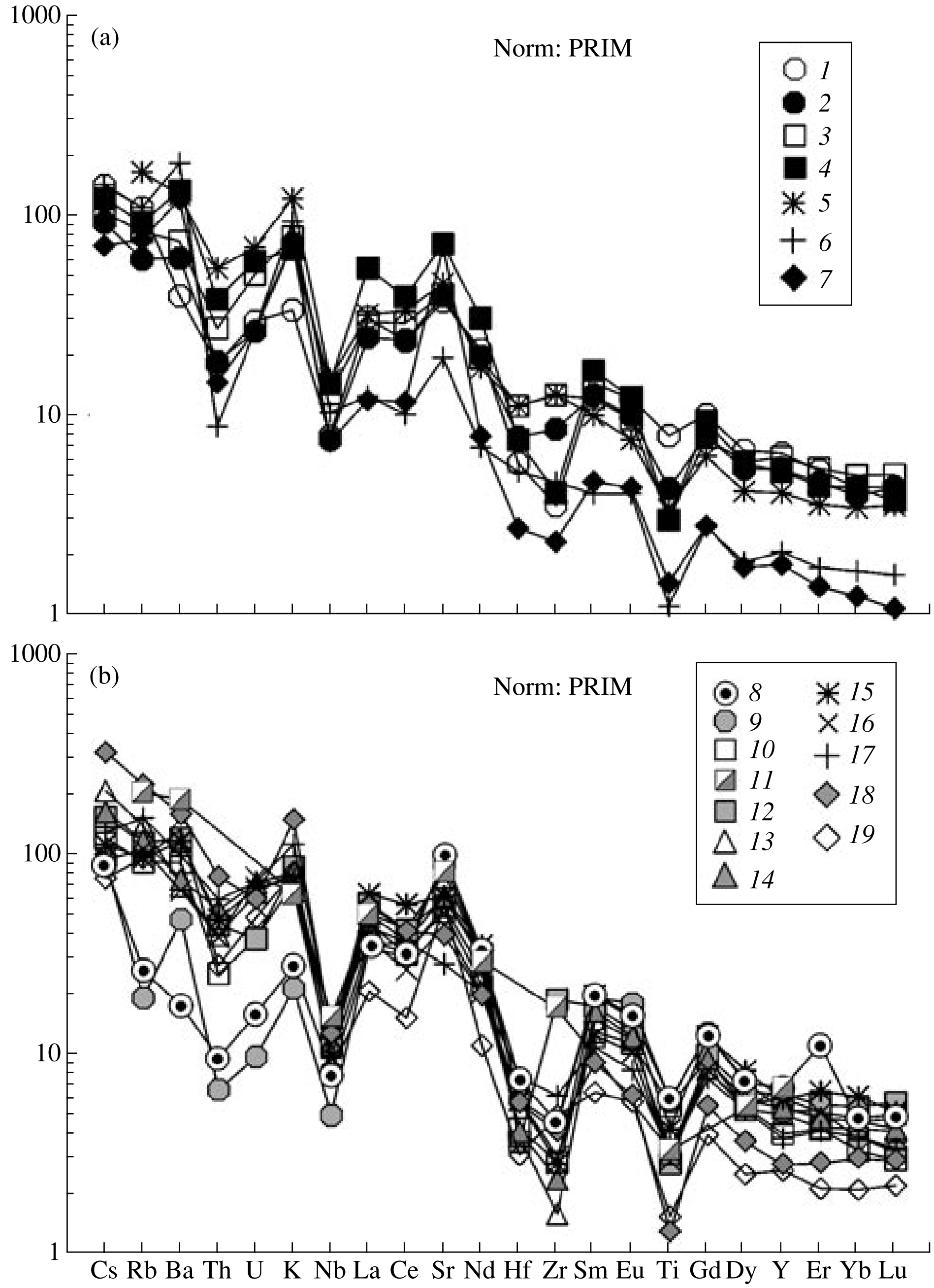

Fig. 1. PM-normalized spidergrams for rocks of the (A) first and second phases and (B) third and fourth phases. Normalizing values are taken from [15]. (*1–19*) Ordinal numbers in Table 2.

melting of the lower crust of the Aldan Shield. This hypothesis is supported by the following arguments.

The generation of compositionally different rocks of the complex is related to independent melts rather than fractional differentiation. Their link to different sources is indicated by the absence of an Eu minimum in all the rock types; insignificant variations in the Rb/Sr ratio; independent trends for different rocks in the Ba–Sr, Rb–K_2O, Cr(Ni)–SiO_2, and other diagrams; the absence of a Zr–Ti correlation; and variations in ratios of incompatible and immobile elements (Ba/Nb, Th/Ta, Zr/Nb). Melts with suprasubduction signatures can be generated not only by fluid enrichment of the mantle wedge above subduction zones but also by repeated melting of basic rocks with extraction of incompatible elements [8] or by partial melting of amphibolites [14]. Hence, the subalkaline rock association of the Ketkap–Yuna province could have been produced by the partial and different-level melting of plagioclase-rich sources (amphibolites, amphibole–plagioclase schists, metadiorites, and plagiogneisses), which are widespread in

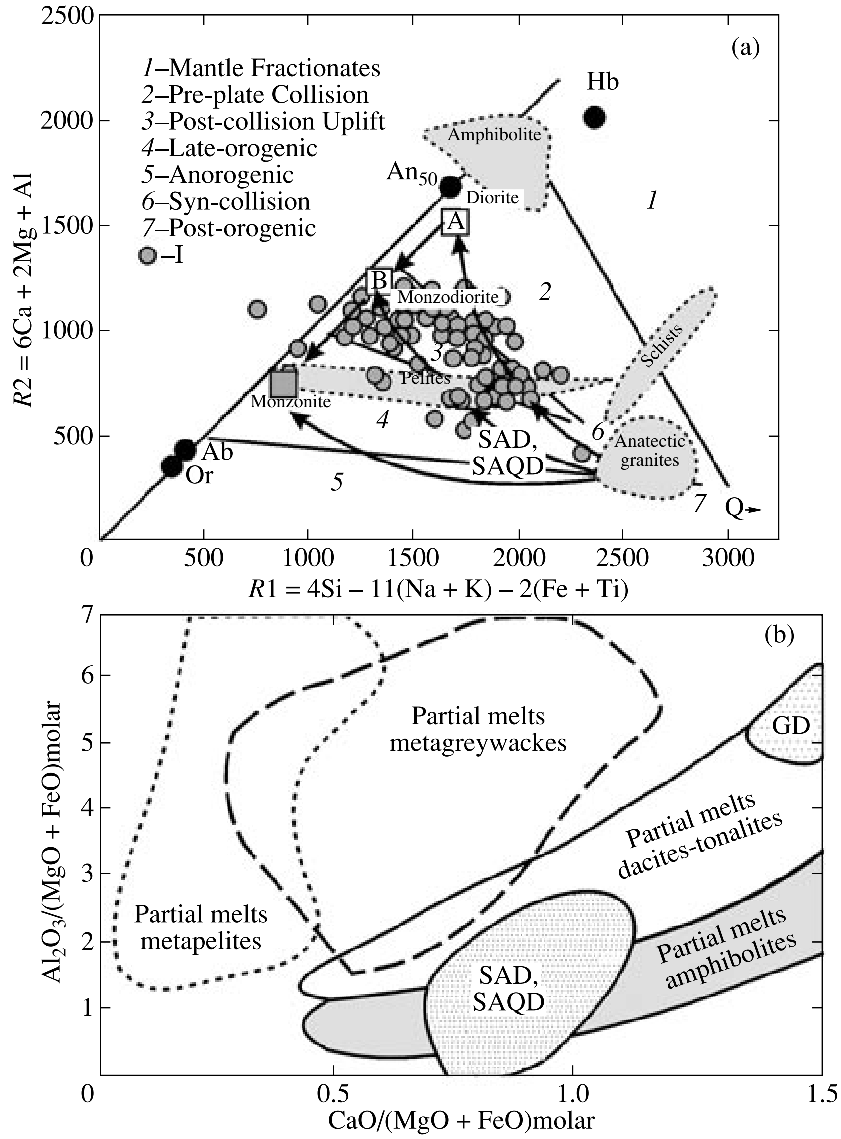

Fig. 2. Fields and curves of partial melting of various metasedimentary and amphibolite sources in the diagrams of (A) Batchelor and Bowden [11] and (B) Gerdes et al. [13]. (I) Rocks of the Uchur Complex. Fields with specks are rocks of the Uchur Complex: (SAD, SAQD) subalkaline diorites and quartz diorites, respectively; (GD) granodiorites and granites.

the crystalline basement of the shield (Fig. 2). This is also suggested by REE patterns, which are similar to those of the tonalite–trondhjemites, disposition of data points in the partial melting curves of the process identification and Sr/Ca–Ba/Ca diagrams, high contents of Al and Ca, and some other characteristics. Only small-volume leucogranite veins, which terminate the fourth stage of the Uchur Complex evolution and exhibit signatures of *S*- and *A*-type granites, can be considered products of either partial melting of metagraywackes or, more probably, of high differentiation (possibly, emanation) of moderately silicic granite melt. The energy (partly, matter as well) consumed during melting was presumably supplied by a deep fluid–thermal flow, which could ascend along columns of mantle-derived alkaline basic magmas.

This conclusion is probably applicable to all granitoids in Mesozoic tectonomagmatic activation zones of the Aldan Shield.

The $^{87}Sr/^{86}Sr$ ratios measured in the rocks of various phases of the Uchur Complex range from 0.704350 to 0.704420 (Table 2) regardless of the evolution sequence and composition. These values are closest to those of the typical mantle-derived rocks. Hence, the formation of rocks of the Uchur Complex is related to upper mantle sources or, more likely, rocks with a short-term crustal history. In the latter case, isotopic–geochemical features of the rocks reflect interaction between essentially mafic (primarily, mantle) crustal protolith and mantle influx. Similar results were obtained for the Sr isotopic composition of diorites and granodiorites of the Ketkap Range [2].

The Uchur Complex of the Ketkap–Yuna province can be considered a product of partial melting of plagioclase-rich rocks at different levels in the course of various stages of a single tectonic cycle related to the existence of a continental transform margin of the Californian type. According to the proposed model, the first stage of tectonomagmatic activation was responsible for the origination of mantle chambers of alkaline basaltic magmas. Together with processes of parataxis and fluid syntaxis, these magmas generated lower crustal chambers of alkali earth melts. At the second stage, increase in the fluid–heat flow owing to the emplacement of the mantle magmas in the earth's crust and corresponding uplift of magma generation front to the higher crustal levels promoted the generation of subalkaline diorites, quartz diorites, granodiorites, and granites, which differed from the rocks of the first stage in higher contents of K and Au. Monzonitoid magmas of the Ketkap Complex were also emplaced at the second stage.

REFERENCES

1. O.A. Bogatikov and A. K. Simon, Herald of the DGGGMS RAS **1** (2) (1997). http://www.scgis.ru/russian/cp1251/dggms/2-97/magma.htm.
2. V. S. Ivanov, in *Proceedings of International (10th All-Russia) Petrographic Conference* (Apatity, 2005), Vol. 1, pp. 84–85 [in Russian].
3. L. M. Parfenov, *Continental Margins and Island Arcs of Mesozoides of Northeast Asia* (Nauka, Novosibirsk, 1984) [in Russian].
4. B. N. Permyakov, in *Proceedings of the 2nd All-Russia Petrographic Conference 2000* (Syktyvkar, 2000), Vol. 1, pp. 159–161 [in Russian].
5. V. F. Polin and E. D. Petrachenko, in *Proceedings of 11th Session of the Northeastern Division of the All-Russia Mineralogical Society* (Magadan, 2001), Vol. 1, pp. 185–191.
6. V. F. Polin and V. G. Sakhno, Dokl. Akad. Nauk **394**, 364 (2004) [Dokl. Earth Sci. **394**, 28 (2004)].
7. V. F. Polin, V. G. Sakhno, and A. N. Solyanik, Dokl. Akad. Nauk **398**, 385 (2004) [Dokl. Earth Sci. **398**, 1001 (2004)].
8. A. D. Saunders and J. Tarney, in *Marginal Basin Geology,* Ed. by B. P. Kokelaar and M. F. Howels (Blackwell, Oxford, 1984; Mir, Moscow, 1987), pp. 59–76.
9. A. I. Khanchuk, V. V. Golozubov, Yu. A. Martynov, and V. P. Simanenko, in *Proceedings of 30th Tectonic Conference. Tectonics of Asia* (Moscow, 1997), pp. 240–243 [in Russian].
10. S. Agrawal, J. Geol. **10**, 529 (1995).
11. R. A. Batchelor and P. Bowden, Chem. Geol. **48**, 43 (1985).
12. B. W. Chappel and A. J. R. White, Pacific Geol. **8**, 173 (1974).
13. A. Gerdes, G. Wörner, and A. Henk, J. Geol. Soc. London **157**, 577 (2000).
14. J. B. Gill, *Orogenic Andesites and Plate Tectonics* (Springer, New York, 1981).
15. D. A. Wood, J. Geol. **7**, 499 (1979).